J. Synchrotron Rad. (1999). **6**, 773–775

Evolution of long-range and short-range order in $La_{0.67}Ca_{0.33}MnO_{3-\delta}$ during solid-state transformation using high-energy ball milling

Shaheen Islam[a], M.B. Liou[b], D.J. Fatemi[c], J.O. Cross[c], V. G. Harris[c], and W. T. Elam[c]

[a] *Virginia Union University, Richmond VA*
[b] *Cornell University, Ithaca, NY*
[c] *U. S. Naval Research Laboratory, Washington, D. C.*

A novel processing scheme has been developed that allows for the single step processing of nanostructured complex oxides. This approach involves the high energy ball-milling (HEBM) of binary oxide precursors to form pure phase complex oxides at low-temperatures. Using this technique we have prepared $La_{0.67}Ca_{0.33}MnO_{3-\delta}$ and studied the evolution of short range and long-range order, using EXAFS and XRD respectively, as a function of milling time during the solid state transformation. Transport properties of the milled perovskites are also discussed.

Keywords: ball-milling; extended x-ray absorption fine structure; colossal magnetoresistance; manganates

1. Introduction

Lanthanum manganite ($LaMnO_3$) is an antiferromagnetic, insulating perovskite that can be driven into a metallic state by replacing a fraction of trivalent La ions by divalent ions. The properties of compounds having Ca and Sr substitutions have been widely reported. As electronic transport becomes possible in these materials, the antiferromagnetic spin order changes from paramagnetic to ferromagnetic. In the neighborhood of their ferromagnetic transition temperature T_C, these manganese perovskites show a dramatic decrease in resistivity with applied magnetic field. This effect has become known as Colossal Magnetoresistance or CMR.(Chahara et al., 1993; vonHelmolt et al., 1993; Jin et al., 1994) Recent studies have shown that the atomic disorder around the Mn cations play a pivotal role in determining the transport and magnetic behavior of this class of materials. (Stroud et al., 1997; Browning et al., 1998) In order to better understand the relationship between local disorder and the CMR phenomenon we have chosen to produce LCMO via a novel technique that incorporates a large degree of atomic disorder in the form of points defects and strain to the end product. Specifically, we employ ball milling where particles of the starting mixture experience repeated high energy collisions that act to fractured and atomically mix their constituent atoms leading to the amorphization and subsequent recrystallization to another phase. In this way, low-temperature solid state reactions are possible.

In this paper we report the evolution of long range and short range order in the solid state transformation of binary oxides to $La_{0.67}Ca_{0.33}MnO_{3-\delta}$ via high-energy ball-milling. X-ray diffraction (XRD) and extended x-ray absorption fine structure (EXAFS) techniques are used to study this evolution. The transport properties of these samples, before and after heat treatment, are also discussed in the context of the atomic structure around the Mn cations.

2. Sample Processing

The samples in this study have been prepared using high energy ball-milling where the starting mixture consists of binary oxides of La_2O_3, CaO, and MnO in a molar ratio of 1:1:3. The ball-milling has been carried out in a Spex shaker mill, Model 8000, using a hardened tool-steel vial and stainless steel balls. We have used two large balls of mass 8 gm and two smaller balls of mass 1 gm. The ball to powder mass ratio was 9:1. The milling duration ranged from 10-40 uninterrupted hours in an air environment.

To minimize point defects introduced during HEBM, the samples have been annealed in air as compacted pellets for soak times of 5 hours. The annealing temperature ranges from 500°C to 1300°C.

A LCMO standard was prepared via traditional fire and grinding techniques to be used as a structural and transport reference to the milled samples. Thermal annealing at 1300° C for 65 hours was found to produce a homogeneous alloy.

3. Evolution of Long-Range Order

In order to examine the time dependence of structural refinement during HEBM, milled mixtures have been analyzed by x-ray diffraction after various milling times and compared with the LCMO standard and the starting material mixture. The diffraction data have been collected at room temperature in the 2θ range of 20° to 120° using a Phillips (vertical θ–2θ) diffractometer with $Cu_{k\alpha}$ source. Figure 1 shows a series of XRD patterns for the samples milled for 0, 20, 30 and 40 hours together with the starting material mixture and the $La_{0.67}Ca_{0.33}MnO_{3-\delta}$ standard (space group *pnma*; a=5.4289Å; b=5.4557Å; c=7.8194Å; vol=231.6Å^3).

In the upper left corner of each data set is a scaling factor which allows meaningful amplitude comparisons between data sets. After 20h of milling, the amplitude of the diffraction features are significantly reduced and some major peaks in the spectra for the starting mixture are absent signaling a reduction in the volume fraction of the precursor binary oxides and the creation of some other intermediate mixed oxide phases. After 30h of milling, all the major diffraction features can be indexed to the LCMO space group having the following unit cell dimensions: a=5.4546Å; b=5.5016Å; c=7.7973Å; vol=234Å^3. Some small features, e.g. at 2θ~35°, indicate that this samples is not a pure phase. However, after 40h of milling the spectra shows no signs of secondary phases and the primary phase lattice parameters are: a=5.4376Å; b=5.4618Å; c=7.8082Å; vol=231.9Å^3, values much closer to that of the reference standard. The unit cell parameters appears to approach those of the LCMO standard with increased milling duration.

In comparing the 40 h milled spectrum to the LCMO standard, one sees that every diffraction feature can be directly correlated to that of the reference compound. Slight shifts in the diffraction peaks relative to those of the standard are believed to be caused by differences in the lattice parameters that we attribute to anion defects in the milled samples.

4. Evolution of Short-Range Order

Extended X-ray Absorption Fine Structure (EXAFS) has been used to study the short range order of $La_{0.67}Ca_{0.33}MnO_{3-\delta}$ powder. The EXAFS data have been

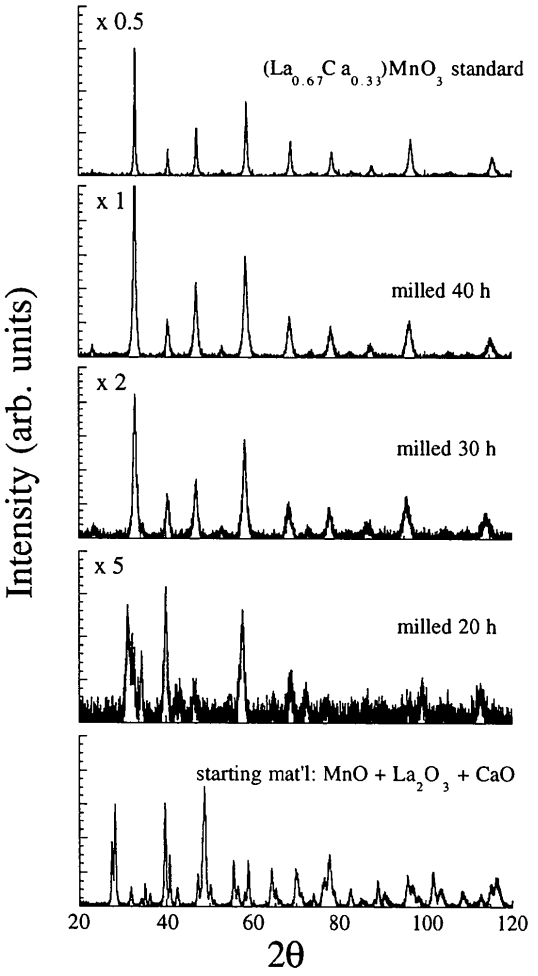

Figure 1. X-ray diffraction spectra collected using Cu k_α radiation for ball-milled mixtures. Similar data from the starting mixture and from a ceramic LCMO standard are also presented. Scaling factors plotted on each panel allow interpretation of amplitude peak amplitudes.

collected using both transmission and fluorescence yield at beam line X23B at the National Synchrotron Light Source.

Due to space constriction we limit our discussions here to only the Mn EXAFS, Mn being the only magnetic ion of the system and therefore integral to the unique magnetotransport properties. Figure 2 is a plot of the x-ray absorption coefficient encompassing the Mn K absorption in the LCMO sample milled for 40h. These data are representative of all other data discussed herein. Following standard EXAFS analysis procedures (Sayers and Bunker, 1988), the fine structure ranging from 28 to 564 eV above the Mn absorption edge were isolated and normalized to the edge energy and step height. A cubic spline was then fit and removed from the data using four equally spaced internal knots to minimize atomic background curvature. These data where then converted to photoelectron wave vector space (k). Figure 3 is a plot of the normalized Mn EXAFS (χ^*k^3). The error bars presented on the data of Fig. 3 represent both the uncertainty related to the statistics of the data collection as well as those introduced to the data during the preceding analysis procedures, most notably, the background removal procedure. A k^3-weighting weighting was applied to a k-range of 3-11.7Å^{-1} for the Fourier transformation. The k-range was prematurely terminated due to Fe contamination of the sample presumably from the ball and cylinder materials.

In Fig. 4 are four panels of Fourier transformed Mn EXAFS data collected from the same set of samples whose XRD data are presented in Figure 1. In the lower three panels the data are plotted with data collected from an MnO standard. This is the atomic environment of the Mn in the starting mixture. The topmost panel is a plot of the 40h milled sample together with the Mn EXAFS collected from the LCMO standard, i.e. the desired end product. The solid curves reflect the the atomic environments around the Mn cations at intermediate stages of processing. The near neighbor anion bond in these data appear at r-values of 1.9Å for the MnO and 1.5-1.6Å for the LCMO. These values have not been corrected for an electron phase shift and hence are not the true bond distances.

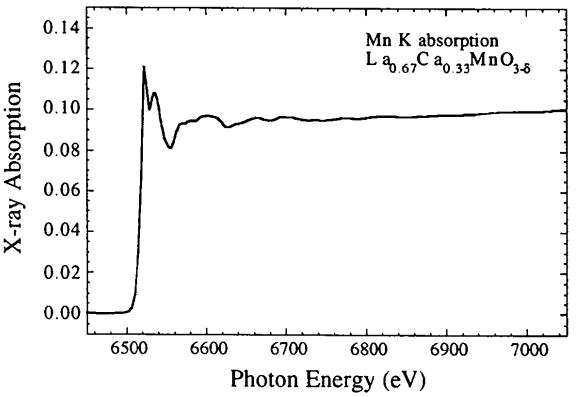

Figure 2. X-ray absorption coefficient as a function of photon energy encompassing the Mn K absorption energy for the ball-milled LCMO (40 hrs.). Data were collected in fluorescence yield mode.

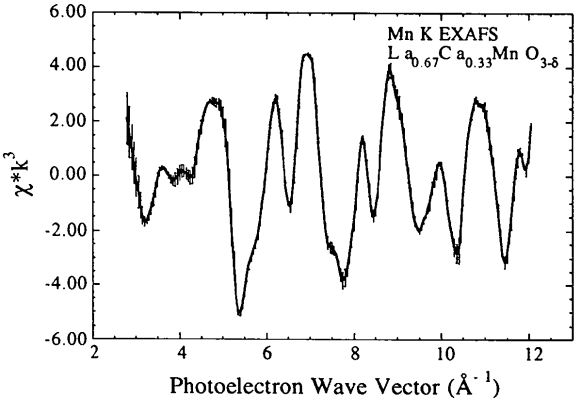

Figure 3. Normalized Mn EXAFS (χ) with error bars representing both the statistical uncertainty in the data collection and that introduced to the data by the background removal procedure.

As one can qualitatively infer, the Mn environment for samples milled for both 20 h and 30 h resemble that of the Mn in the MnO phase. This is evidenced by the radial distance and relative amplitudes of the Fourier peaks. Note that the peak amplitudes in the sample milled for 30h are much lower than those of the MnO standard signaling the increased atomic disorder that accompanies the continued milling and gradual amorphization of the starting mixture.

However, it is not until 40 h of milling that one observes directly a change in the local atomic arrangements around the Mn cations from that of the MnO phase to that of the LCMO.

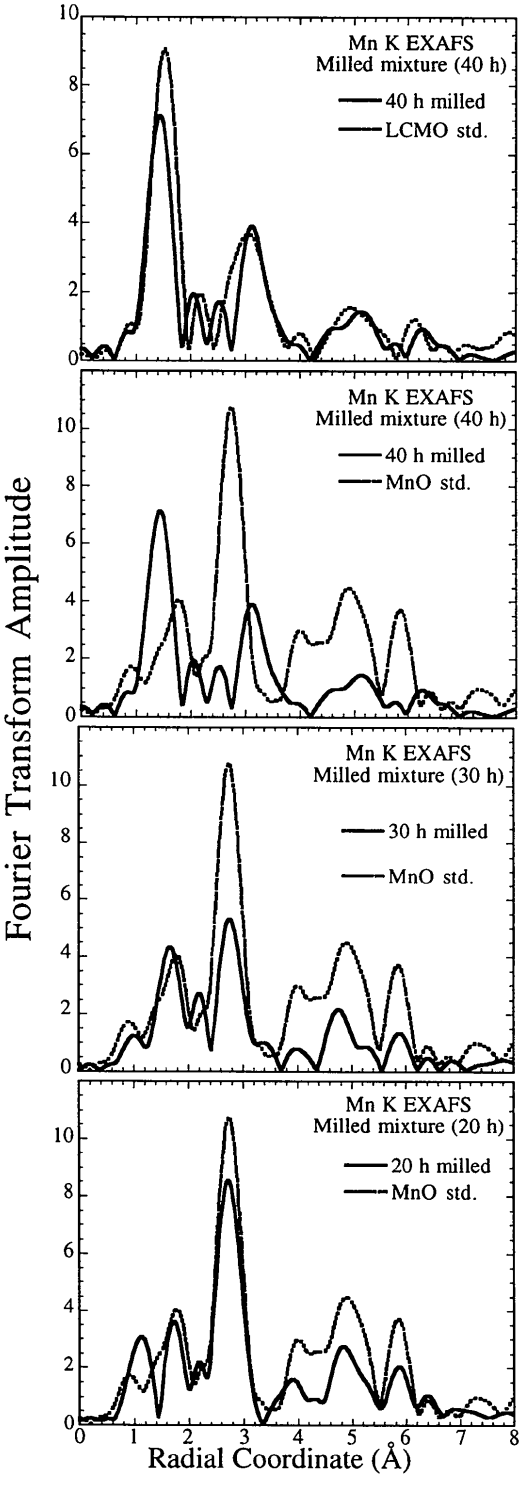

Figure 4. Fourier transformed Mn EXAFS data for the sample mixtures milled for times 20h, 30h and 40h. In each panel their are presented similar data from empirical standards (either MnO or LCMO).

This is most noticeable in the shift of the NN anion peak from the 1.9Å (MnO) to the ~1.5Å for the LCMO, but is also reflected in the amplitude and radial position of higher order peaks. For example, the NN cation peak shifts from ~2.7Å to ~3.2Å.

For milling times up to and including 30h, the Mn EXAFS of Fig. 4 shows unambiguously that the Mn cations reside primarily in the MnO phase. This sample has Fourier peak amplitudes that are significantly depressed compared to the standard. This is consistant with the MnO phase existing in nanoparticle form or at the grain boundaries.

In contrast, the XRD data for the same sample shows that the dominant phase is that of a perovskite having lattice parameters similar to that of LCMO. Because the B-site cation (i.e. Mn) octahedra provide the framework for the LCMO perovskite structure, these results can only be reconciled if the perovskite phase present after 30h of milling has another divalent ion substituting for the B-site cation. The likely candidate is Ca^{+2}, but the contamination of Fe from the canister and ball materials may also fulfill this role if the contamination is severe and is incorporated as divalent Fe in the perovskite.

Magnetization data as a function of temperatureindicate that the sample is in a paramagnetic (P) state for T>150K and a ferromagnetic (F) state for T<150K. This P-F transition is fully consistent with previous findings for doped LMO samples (Schiffer et al., 1995). However, the transport properties of these samples reveal no insulator-to-metal (I-M) transition which is expected to occur simultaneous with the P-F transition. Recently, researchers at the NRL have studied a large body of LCMO samples and concluded that the magneto-transport properties of this class of materials is strongly influenced by disorder introduced during processing.(Stroud et al., 1997; Browning et al., 1998) When the disorder is increased in a controlled fashion, for example via ion radiation damage, the I-M transition is shifted to lower temperatures until finally it is suppressed. We attribute the suppression of the I-M transition in our samples to anion defects.

The Fourier transformed Mn EXAFS from annealed samples (not shown) have nearly identical transform profiles to that of the LCMO standard. However, the NN anion peak is still ~10% smaller in amplitude for all annealed samples regardless of annealing temperature. This heat treatment is expected to be effective in relieving stress in the samples but may not provide sufficient thermal energy for annihilating anion defects.

This work was performed, in part, at the National Synchrotron Light Source, which is sponsored by the U.S. Department of Energy. At the time of this research S. Islam was supported as an ASEE-NAVY summer fellow, and D.J. Fatemi and J.O.Cross. were supported as NRC/NRL postdoctoral fellows.

References

Browning, V.M., et al. (1998). *J. Appl. Phys.* **83**(11), 7070.
Chahara, K., et al. (1993). *Appl. Phys. Lett.* **63**, 1990.
Jin, S., et al. (1994). *Science* **264**, 413.
Sayers, D.E. and Bunker, B.A. (1988). Data Analysis. X-ray Absorption: Principles, Applications, Techniques of EXAFS, SEXAFS, and XANES. D. C. Koningsberger and R. Prins. New York, John Wiley & Sons. **92:** 211-253.
Schiffer, P., et al. (1995). *Phys. Rev. Lett.* **75**, 3336.
Stroud, R.M., et al. (1997). Effects of Radiation Induced Disorder in $La_{1-x}Ca_xMn_yO_3$ Thin Films. Metallic Magnetic Oxides. J. N. M. Hundley, R. Ramesh, Y. Tokura. Boston, Mater. Res. Soc. Symp. Proc.: 494.
von Helmolt, R., et al. (1993). *Phys. Rev. Lett.* **71**, 2331.

(Received 10 August 1998; accepted 1 December 1998)